chemosensors

MDPI

Supporting Information

Influence of pH on Room-Temperature Synthesis of Zinc Oxide Nanoparticles for Flexible Gas Sensor Applications

Fazia Mechai [1,2,3], Ahmad Al Shboul [1,*], Mohand Outahar Bensidhoum [2,3], Hossein Anabestani [4], Mohsen Ketabi [1] and Ricardo Izquierdo [1,*]

[1] Department of Electrical Engineering, École de Technologie Supérieure (ETS), 1100 Notre-Dame St W, Montreal, QC H3C 1K3, Canada; fazia.mechai.1@ens.etsmtl.ca (F.M.); mohsen.ketabi.1@ens.etsmtl.ca (M.K.)
[2] Artificial Vision and Automatic Systems (LVAAS) Laboratory, Mouloud Mammeri University of Tizi-Ouzou (UMMTO), Tizi Ouzou, C1063600 Algeria; mohand-outahar.bensidhoum@ummto.dz (M.O. B.)
[3] Faculty of Electrical and Computer Engineering, Mouloud Mammeri University Tizi-Ouzou (UMMTO), Tizi Ouzou 15000, Algeria
[4] Department of Electrical Engineering, McGill University, 845 Sherbrooke St W, Montreal, QC H3A 0G4, Canada; hossein.anabestani@mail.mcgill.ca (H.A.)
* Correspondence: ahmad.al-shboul@etsmtl.ca (A.A.S.); ricardo.izquierdo@etsmtl.ca (R.I.)

Citation: Mechai, F.; Al Shboul, A.; Bensidhoum, M.O.; Anabestani, H.; Ketabi, M.; Izquierdo, R. Influence of pH on Room-Temperature Synthesis of Zinc Oxide Nanoparticles for Flexible Gas Sensor Applications. *Chemosensors* **2024**, *12*, 83. https://doi.org/10.3390/chemosensors12050083

Received: 31 March 2024
Revised: 3 May 2024
Accepted: 7 May 2024
Published: 21 May 2024

Nextronmicroprobe station (Peltier-type sample stage, Seoul, Republic of Korea)

The Nextronmicroprobe station (**Figure S1(A,B)**) with a Peltier-type sample stage, developed in Korea [1], provides a versatile platform for the electrical characterization of samples under controlled temperature, gas, and humidity conditions.

The probe station can accommodate up to six probes made of a rhodium material that can be connected to the sample. The probe station allows for monitoring the sensors' electrical resistance measurements during experiments with a programmed multimeter connected to a PC via an Arduino card. The stage size is typically around 19 mm × 19 mm and made of rhodium-coated copper, which controls heat between −40 °C and + 170 °C with an average ramp speed of up to 60°C min^{-1}. The probe station also offers optional gas dosing and humidity control capabilities during experiments. The humidity control system can be in the normal range between relative humidity (RH) of 4% and 95% and has an average ramp speed of 10% $RHmin^{-1}$. A humidity sensor is installed inside the chambers to monitor RH during experiments. The chamber has gas flow control for precise and stable flow control. The gas flow station, built with the mass flow control unit, gas flow pipeline, and electrical components, is the ideal solution for various applications demanding precise and stable flow control.

The Nextron probe station can generate and control humidity as it is equipped with a humidity control system (HCS). This system consists of a two-channel Mass Flow Controller (MFC) that can precisely control the flow of dry and humid gas into the probe station chamber. The probe station has a humidity sensor installed inside the chamber, allowing the system to monitor and precisely control the humidity levels within the chamber.

The HCS generates humid gas by passing a dry gas, such as nitrogen or air, through a water bubbler or other humidification device (**Figure S1(C)**). This saturates the gas with water vapor, which can then be precisely mixed with the dry gas using the MFC to achieve the desired humidity level. The HCS uses feedback from the humidity sensor to automatically adjust the mixing ratio of dry and humid gas to maintain the target humidity level within the chamber. This allows for the tight control and stabilization of the humidity environment.

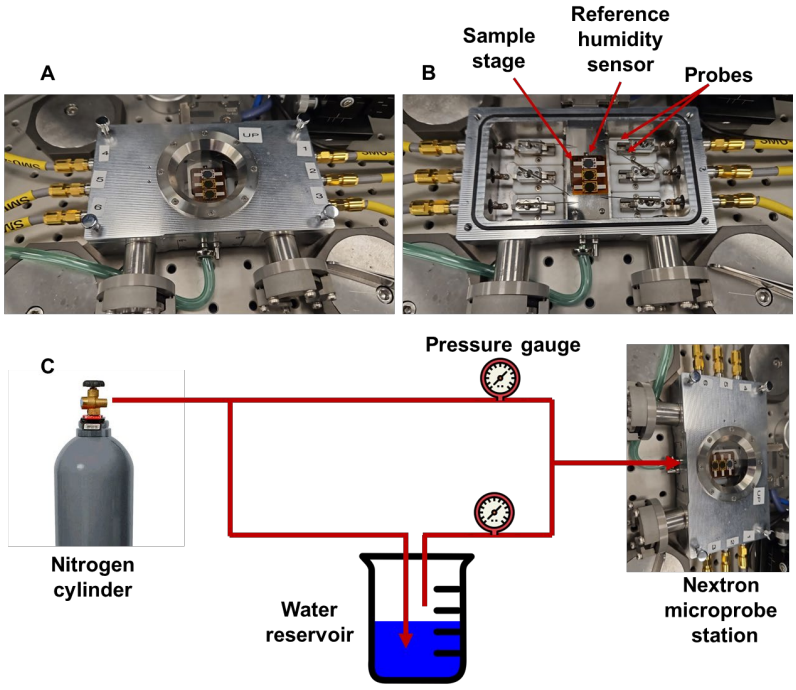

Figure S1. (**A**,**B**) The Nextronmicroprobe station with a Peltier-type sample stage. (**C**) Schematic illustration of humidity generation in the Nextron station with the humidity control system (HCS).

Lab-made organic solvent gas generator

We used a lab-made organic solvent gas generator. Imagine a device comprising a heated flask and a coil submerged in a cooling bath. Inside the flask, a chosen organic solvent awaits its transformation. As the temperature within the flask rises, controlled by a precise heat source, the solvent evaporates. We used mass flow meters to measure the amount of solvent vaporized, ensuring consistent and repeatable experiments. By monitoring the mass flow rate of the vapor leaving the heated flask, we could adjust the heating or cooling parameters to achieve the target concentration. This heated vapor then ascends into a serpentining coil bathed in a coolant. The vapor encounters a resistance by maintaining a precise coolness within the coil. This thermal opposition condenses some vapor into liquid form, effectively concentrating the organic solvent gas stream. The remaining uncondensed vapor, now boasting a heightened purity and a specific concentration thanks to the thermal control, continues its journey to the Nextron chamber.

Table S1. Literature overview of recent ZnO NMs employed in the development of gas sensors.

ZnO morphologies	Synthesis technique	Substrate	Gas	Concentration (ppm)	Operating temperature (°C)	Response	Response time (s)	Recovery time (s)	Ref
ZnO Nanoparticles	Co-precipitation	Glass	NH_3	50	RT	7.29	46	29	[2]
ZnO:Eu Nanowire	Electrochemical	FTO/ glass	H_2	100	RT	2.1	7	42	[3]
Ni-ZnO Nanorods	Hydrothermal	FTO	H_2S	5	250	68.9%	75	54	[4]
ZnO/Mn-PY Nanofiber	Hydrothermal	Core yarn (PY)	NH_3	100	RT	13.13	64	24	[5]
ZnO Nanoparticles	Sonication	Si/SiO_2	CO	40	RT	23.7%	-	-	[6]
ZnO/LIG Nanorods	Hydrothermal	polyimide (PI)	NO_2	1	RT	251.71%	9.5	8.3	[7]
Ag–ZnO/GO Nanorods	Hydrothermal	FTO	C_2H_2	100	250	187.34%	13	780	[8]
ZnO Nanorods	CBD	SiO2/p-Si	NH3	50	RT	226%	14	4	[9]
Au-ZnO/Mi Crospheres	Hydrothermal	polyimide (PI)	Ethanol	100	320	75.185	-	-	[10]
Pd-ZnO Hexagonal Mi-crodisks	Hydrothermal	Al_2O_3 ceramic	NH3	50	230	3.9	23.2	271.8	[11]

GO/ZnO Thin film	DC reactive sputtering	Glass	NH3	25	RT	14.783	114	21	[12]
ZnO Thin Film	Electron beam deposition	Si and Al_2O_3	O_3	55–1150 ppb	RT	-	<2	<15	[13]
Pt/Pd-decorated WS2-ZnO Nanosheets	Atomic layer deposition	-	Acetone	10	RT	13.77	-	-	[14]

Table S2. Literature overview of recent procedures to synthesize ZnONMs.

ZnO Nanostructure	Method	Precursor-Salt	Reacting Agent	pH	Synthesis Tempera-ture (°C)	Calcination Temperature (°C/hour)	Particle Size (nm)	Band gap Eg(eV)	Applications	Ref
Nanoparticles	Ultrasound / Sol-gel	Zinc acetate	Oxalic acid	-	60	400–700/2	22–30	3.269–3.359	Photocatalytic and antibacterial	[15]
Nanorods	Sol-gel / Hydrothermal	Zinc acetate	Ethanolamine HMTA	-	60 90	-	27.41	-	Power generators and sensors	[16]
Nanoparticles	Sol-gel / Biosynthesis	Zinc acetate	NaOH	-	80 – 60	250/4	-	3.23 – 3.25	Photocatalytic and antibacterial	[17]
Nanoparticles	Biosynthesis	Zinc acetate	NaOH	10–14	90	-	66.47	3.33–3.39	Breast cancer	[18]
Nanoparticles	Biosynthesis / Hydrothermal	Zinc nitrate	Lemon extract	8	180	500/4	-	3.20	Photocatalysis and antibiotics	[19]
Nanosheets	Hydrothermal / Microwave irra-diation	Zinc nitrate	Urea	-	180	500/5	2.32 ± 0.40	3.22	Ethyl sulfide gas sensor	[20]
Nanorods	Magnetron sputtering	Zinc nitrate	Methenamine	-	95	600/1	~50	-	Ethanol gas sensor	[21]
Nanowire	Drop coating / Hydrothermal	Zinc nitrate	HMTA	-	95	400/1	-	-	Hydrogen sulfide gas sensor	[4]
Nanoflowers	Sonochemical	Zinc acetate	KOH	-	RT	-	-	-	DNA biosensors	[22]

Nanoplatelets	Electrodeposition	Zinc chloride	KOH	-	RT	-	3–6	3.11	Solar cells	[23]
Nanoflakes	Hydrothermal	Zinc nitrate	HMTA	-	110	400/2	46	-	Hydrogen sulfide Gas sensor	[24]
Nanowire	Electrochemical deposition	Zinc nitrate	DMAB	9–11	50–80	400/1	-	3.27	Photocatalytic watertreatment	[25]
Nanowire	Solvothermal	Zinc acetate	NaOH	-	150	-	12.96	3.18	Photocatalysis	[26]

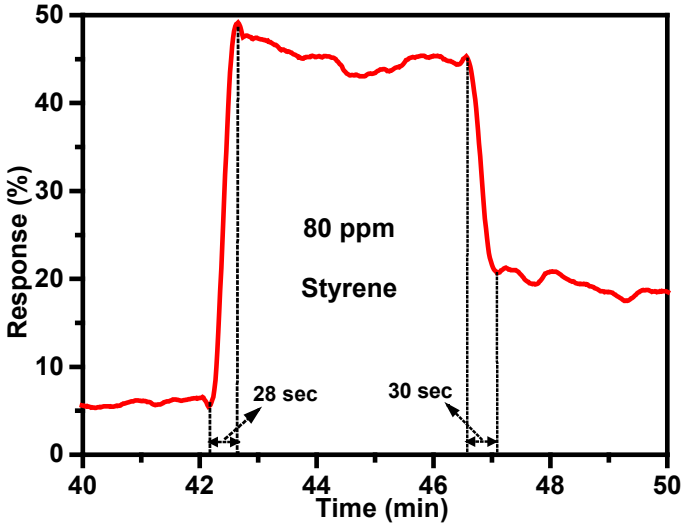

Figure S2. The response to an 80 ppm C8H8 gas concentration provides insights into the response and recovery times.

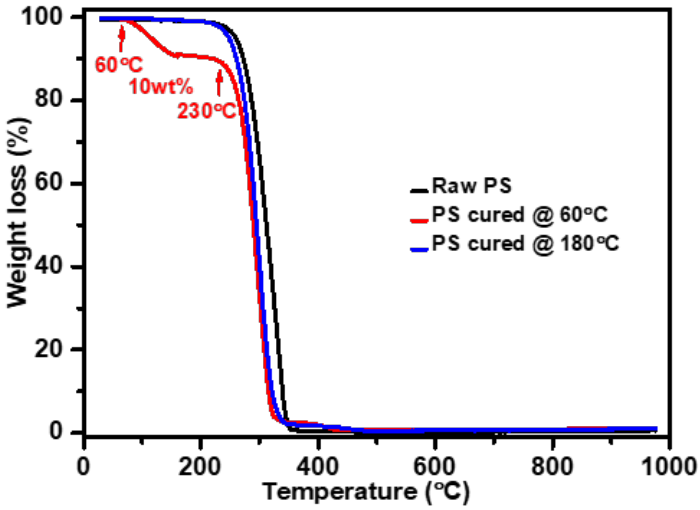

Figure S3. TGA thermograms of raw PS, and PS films cured at 60°C and 180°C.

References

1. Nextron Available online: https://www.microprobesystem.com (accessed on 2 May 2024).
2. Himabindu, B.; Latha Devi, N.S.M.P.; Nagaraju, P.; Rajini Kanth, B. A Nanostructured Al-Doped ZnO as an Ultra-Sensitive Room-Temperature Ammonia Gas Sensor. *J Mater Sci: Mater Electron* **2023**, *34*, 1014, https://doi.org/10.1007/s10854-023-10337-6.
3. Lupan, C.; Mishra, A.K.; Wolff, N.; Drewes, J.; Krüger, H.; Vahl, A.; Lupan, O.; Pauporté, T.; Viana, B.; Kienle, L.; et al. Nanosensors Based on a Single ZnO: Eu Nanowire for Hydrogen Gas Sensing. *ACS Appl Mater Interfaces* **2022**, *14*, 41196–41207, https://doi.org/10.1021/acsami.2c10975.
4. Liu, S.; Yang, W.; Liu, L.; Chen, H.; Liu, Y. Enhanced H2S Gas-Sensing Performance of Ni-Doped ZnO Nanowire Arrays. *ACS omega* **2023**, *8*, 7595–7601, https://doi.org/10.1021/acsomega.2c07092.
5. Lin, J.-H.; Yang, T.; Zhang, X.; Shiu, B.-C.; Lou, C.-W.; Li, T.-T. Mn-Doped ZnO/SnO2-Based Yarn Sensor for Ammonia Detection. *Ceram. Int.* **2023**, *49*, 34431–34439, https://doi.org/10.1016/j.ceramint.2023.07.222.
6. Daniel, T.T.; Yadav, V.K.S.; Abraham, E.E.; Paily, R.P. Carbon Monoxide Sensor Based on Printed ZnO. *IEEE Sens. J.* **2022**, *22*, 10910–10917, https://doi.org/10.1109/JSEN.2022.3166811.
7. Tseng, S.-F.; Chen, P.-S.; Hsu, S.-H.; Hsiao, W.-T.; Peng, W.-J. Investigation of Fiber Laser-Induced Porous Graphene Electrodes in Controlled Atmospheres for ZnO Nanorod-Based NO2 Gas Sensors. *Appl. Surf. Sci.* **2023**, *620*, 156847, https://doi.org/10.1016/j.apsusc.2023.156847.
8. Kamble, C.; Narwade, S.; Mane, R. Detection of Acetylene (C2H2) Gas Using Ag-Modified ZnO/GO Nanorods Prepared by a Hydrothermal Synthesis. *Mater. Sci. Semicond. Process.* **2023**, *153*, 107145, https://doi.org/10.1016/j.mssp.2022.107145.
9. Kumar, B.B.; Bhowmik, B.; Singh, A.P.; Jit, S.; Singh, K. Room Temperature ZnO Nanorods Based TFT Ammonia Sensor: An Experimental and Simulation Study. *Appl. Phys. A* **2024**, *130*, 308, https://doi.org/10.1007/s00339-024-07474-y.
10. Chao, J.; Meng, D.; Zhang, K.; Wang, J.; Guo, L.; Yang, X. Development of an Innovative Ethanol Sensing Sensor Platform Based on the Construction of Au Modified 3D Porous ZnO Hollow Microspheres. *Mater. Research Bull.* **2024**, *170*, 112569, doi:10.1016/j.materresbull.2023.112569.
11. Li, Y.; Zhang, B.; Li, J.; Duan, Z.; Yang, Y.; Yuan, Z.; Jiang, Y.; Tai, H. Pd-Decorated ZnO Hexagonal Microdiscs for NH3 Sensor. Chemosensors 2024, 12, 43. https://doi.org/10.3390/chemosensors12030043.
12. Natarajamani, G.S.; Kannan, V.P.; Madanagurusamy, S. Synergistically Enhanced NH3 Gas Sensing of Graphene Oxide-Decorated Nano-ZnO Thin Films. *Mater. Chem. Phys.* **2024**, 129036, https://doi.org/10.1016/j.matchemphys.2024.129036.
13. Bolli, E.; Fornari, A.; Bellucci, A.; Mastellone, M.; Valentini, V.; Mezzi, A.; Polini, R.; Santagata, A.; Trucchi, D.M. Room-Temperature O3 Detection: Zero-Bias Sensors Based on ZnO Thin Films. *Crystals* **2024**, *14*, 90, https://doi.org/10.3390/cryst14010090.
14. Kim, J.-Y.; Mirzaei, A.; Lee, M.H.; Kim, T.-U.; Kim, S.S.; Kim, J.-H. Boosting the Acetone Gas Sensing of WS2–ZnO Nanosheets by Codecoration of Pt/Pd Nanoparticles. *J. Alloys Compd.* **2024**, 174325, https://doi.org/10.1016/j.jallcom.2024.174325.
15. Nguyena, N.; Nguyen, V. Ultrasound-Assisted Sol-Gel Synthesis, Characterization, and Photocatalytic Application of ZnO Nanoparticles. *Dig. J. Nanomater. Biostruct.* **2023**, *18*, 889–897, https://doi.org/10.15251/DJNB.2023.183.889.
16. Torres, F. del C.G.; López, J.L.C.; Rodríguez, A.S.L.; Gallardo, P.S.; Morales, E.R.; Hernández, G.P.; Guillen, J.C.D.; Flores, L.L.D. Sol–Gel/Hydrothermal Synthesis of Well-Aligned ZnO Nanorods. *Bol. Soc. Esp. Ceram. Vidrio* **2023**, *62*, 348–356.
17. Haque, M.J.; Bellah, M.M.; Hassan, M.R.; Rahman, S. Synthesis of ZnO Nanoparticles by Two Different Methods & Comparison of Their Structural, Antibacterial, Photocatalytic and Optical Properties. *Nano Express* **2020**, *1*, 010007, https://doi.org/10.3390/cryst12081142.
18. Al Awadh, A.A.; Shet, A.R.; Patil, L.R.; Shaikh, I.A.; Alshahrani, M.M.; Nadaf, R.; Mahnashi, M.H.; Desai, S.V.; Muddapur, U.M.; Achappa, S.; et al. Sustainable Synthesis and Characterization of Zinc Oxide Nanoparticles Using Raphanus Sativus Extract and Its Biomedical Applications. *Crystals* **2022**, *12*, 1142.
19. Batterjee, M.G.; Nabi, A.; Kamli, M.R.; Alzahrani, K.A.; Danish, E.Y.; Malik, M.A. Green Hydrothermal Synthesis of Zinc Oxide Nanoparticles for UV-Light-Induced Photocatalytic Degradation of Ciprofloxacin Antibiotic in an Aqueous Environment. *Catalysts* **2022**, *12*, 1347. https://doi.org/10.3390/catal12111347.
20. Lee, M.; Kim, M.Y.; Kim, J.; Park, C.O.; Choa, H.E.; Lee, S.Y.; Park, M.K.; Min, H.; Lee, K.H.; Lee, W. Conductometric Sensor for Gaseous Sulfur-Mustard Simulant by Gold Nanoparticles Anchored on ZnO Nanosheets Prepared via Microwave Irradiation. *Sens. Actuators B: Chem.* **2023**, *386*, 133726, https://doi.org/10.1016/j.snb.2023.133726.
21. Yan, P.; Hu, Q.; Chen, J.; Zhou, N.; Zhang, Q. Gas Sensing Property of ZnO NR Arrays Stabilized by High-Temperature Annealing and the Mechanism of Detecting Reduce Gases. *J. Phys. Chem. Solids* **2023**, 111488.
22. Findik, M. ZnO Nanoflowers Modified Pencil Graphite Electrode for Voltammetric DNA Detection and Investigation of Gemcitabine–DNA Interaction. *Mater. Chem. Phys.* **2023**, *307*, 128117, https://doi.org/10.1016/j.matchemphys.2023.128117.
23. Ahmad, H.; Naderi, N.; Yasin, M. Design and Photovoltaic Performance Analysis of Electrodeposited ZnO Microspheres/p-Si Heterojunction Energy Harvesters. *J. Mater. Sci. Mater. Electron.* **2023**, *34*, 414, https://doi.org/10.1007/s10854-023-09851-4.
24. Nakate, U.T.; Yu, Y.-T.; Park, S. Hydrothermal Synthesis of ZnO Nanoflakes Composed of Fine Nanoparticles for H2S Gas Sensing Application. *Ceram. Int.* **2022**, *48*, 28822–28829, https://doi.org/10.1016/j.ceramint.2022.03.017.

25. Manzano, C.V.; Philippe, L.; Serrà, A. Recent Progress in the Electrochemical Deposition of ZnO Nanowires: Synthesis Approaches and Applications. *Crit. Reviews. Solid State. Mater. Sci.* **2022**, *47*, 772–805, https://doi.org/:10.1080/10408436.2021.1989663.
26. Sampath, S.; Rohini, V.; Chinnasamy, K.; Ponnusamy, P.; Thangarasau, S.; Kim, W.K.; Shkir, M.; Maiz, F.; others Solvothermal Synthesis of Magnetically Separable Co–ZnO Nanowires for Visible Light Driven Photocatalytic Applications. *Phys. B Condens. Matter.* **2023**, *652*, 414654, https://doi.org/10.1016/j.physb.2023.414654.